BUCKLING OF SANDWICH BEAMS USING THE EXTENDED HIGH-ORDER SANDWICH PANEL THEORY AND COMPARISON WITH ELASTICITY

C. Phan[1*], G. Kardomateas[1], Y. Frostig[2]
[1] Department of Aerospace Engineering, Georgia Institute of Technology, Atlanta, GA, USA,
[2] Civil and Environmental Engineering, Technion Israel Inst of Technology, Haifa 32000, Israel
* Corresponding author (phanc@gatech.edu)

Keywords: *sandwich composites, buckling, wrinkling, high- order theory*

1 Introduction

Sandwich composites are a unique composite lay-up that consists of two stiff metallic or composite thin face sheets separated by a thick core of low density. This configuration gives the sandwich material system high stiffness and strength with little resultant weight penalty. Classical structural theories neglect the transverse and shear deformation of the core while experimental results [1] have shown non-neglible core compression, and shear failure modes in the core to occur under blast loading. Several sandwich panel theories exist that make various assumptions to better model the core. The differences in these theories is that they either take into account or neglect the axial, transverse normal, or shear stiffness of the core. With regard to buckling, Allen's thick formulation takes into account the core's shear stiffness only [5]. The High-Order Sandwich Panel theory (HSAPT) [2] takes into account the core's transverse and shear stiffnesses, while the Extended Higher Order Sandwich Panel Theory (EHSAPT) takes into account the axial, transverse, and shear stiffnesses in the core [4]. In this paper, the characteristics of the EHSAPT are presented and the equations that determine the critical load for a general asymmetric geometry and different face sheet material are presented. The case study of a simply supported (S-S) sandwich beam undergoing uniform strain/edge beam loading with symmetric geometry and same face sheet materials is used to compare the predicted critical load given by Allen, HSAPT, and EHSAPT to Elasticity [3]. Three solution approaches using EHSAPT were conducted to explore simplifying the loading condition to concentrated loads applied to the face sheet, and including/excluding nonlinear axial strains in the core. Global buckling is studied, followed by wrinkling.

2 Characteristics of EHSAPT

The EHSAPT was recently formulated in [4] based on variational principles. The main characteristics of the EHSAPT are the following:

- 7 generalized coordinates are used to model the displacement field of the sandwich composite: $u_0^t, w_0^t, u_0^c, \phi_0^c, w_0^c, u_0^b, and\ w_0^b$ where the superscripts {*t, b, c*} indicate the lay-up as either top, bottom, or core, respectively; *u* and *w* indicate the axial and transverse displacement of the given lay-up, respectively; ϕ indicates rotation; and the subscript *0* indicates that the location of the generalized coordinate occurs at the midsection of the respective lay-up.
- Face sheets are Euler-Bernoulli type beams. The core has polynomial displacement fields; up to $O(z^3)$ and $O(z^2)$ for the axial and transverse displacement fields, respectively, where 'z' is the through the thickness coordinate. Displacement fields satisfy all interface conditions
- 7 coupled differential equations govern the behavior of the sandwich of total order 18. In order to predict global buckling phenomenon, nonlinear axial strains in the face sheets were considered. Nonlinear axial strains in the core were also considered but were found to not significantly change the accuracy of predicting the critical load in

the global buckling case study. Nonlinear axial strains cause two of the differential equations to be nonlinear.

- 18 boundary conditions result from the variational principle, 9 at each end.

3 Buckling of a S-S sandwich beam

An Elasticity solutions exists to predict the critical global buckling [3] and wrinkling [6] loads of a S-S sandwich beam undergoing compressive loading through an edge beam. In the following sections, we list the formulas for global buckling of sandwich columns from Allen, HSAPT, and EHSAPT (3 cases), give global bucking results that compare these theories to the Elasticity solution given in [3], and then give wrinkling results that compare HSAPT and EHSAPT (1 case) to the Elasticity solution given in [6].

3.1 Allen's formulation and HSAPT

Allen's thick face sheet formulation accounts for the shear rigidity of the core and is given as equation (12) in [3]. HSAPT accounts for transverse normal and shear stiffness in the core. The critical buckling load for a S-S beam with compressive loads applied to the face sheets was solved using HSAPT in [2]. Some algebraic manipulation of equation (82) in [2] leads to HSAPT's asymmetric global buckling load, written in a form similar to Allen:

$$P_{cr_HSAPT} = \frac{P_{E2}\left(1+\mu\left(\frac{P_{Ef}}{P_c} - \frac{P_{Ef}^{\ 2}}{P_c\ P_{E2}}\right)\right)}{1+\mu\left(\frac{P_{E2}-P_{Ef}}{P_c}\right)} \tag{1}$$

where,

$$\mu = 1 + \frac{(2c)^2 G_{xz}^c \pi^2}{12 E_z^c a^2} \tag{2}$$

As $E_z^c \to \infty$, HSAPT reduces to Allen. For long beams (i.e. large length-to-the-total-core-thickness ratio squared $(a/(2c))^2$), the contribution from the E_z^c term is small. The definition of P_{E2}, P_{Ef}, and P_c are given in [3]. For wrinkling, equation (76) in [2] was used.

3.2 EHSAPT (3 cases)

EHSAPT takes into account the axial, transverse normal, and shear rigidity of the core. We have used the EHSAPT to solve three cases: (a) axial load applied exclusively to the top and bottom face sheets and linear axial strain in the core; (b) uniform axial strain applied through the entire thickness and, again, linear axial strain in the core; and (c) uniform axial strain applied through the entire thickness but with nonlinear axial strain in the core, whereas HSAPT was solved using just Case (a). The three cases were chosen to investigate the effect of the different loading conditions and excluding and including nonlinear axial strain in the core. A perturbation approach was used to solve for each case. Buckling using EHSAPT was also presented in [7] where a numerical solution was given, but is now solved using the perturbation approach and compared to Elasticity in this paper.

Case (a): The critical load for concentrated loading just on the face sheets can be determined by finding the value of P for which the perturbed system has a nontrivial solution, or finding P by zeroing the determinant:

$$\det\{[K_{LC}] - \frac{\pi^2}{a^2}\lfloor G_a \rfloor [I]\} = 0 \tag{3}$$

K_{LC} contains stiffness and material constants for a sandwich with linear axial strains in the core. K_{LC} also appears in Case (b) and (c). G_a contains the loading per unit width parameter P. K_{LC} and G_a are given in the Appendix.

Case (b): The critical load for Uniform strain loading with linear axial strains in the core can be determined by finding P from the following perturbed characteristic equation:

$$\det\{[K_{LC}] - \frac{\pi^2}{a^2}\lfloor G_b \rfloor [I]\} = 0 \tag{4}$$

G_b contains the loading per unit width which only has contributions from the face sheets (see Appendix). This is because without nonlinear

axial strain the core, the load parameter on the core will not show up in the perturbed equations.

Case (c): The critical load for edge beam loading which includes nonlinear axial strain in the core:

$$\varepsilon_x^c = \frac{\partial u^c}{\partial x} + \frac{1}{2}\left(\frac{\partial w^c}{\partial x}\right)^2 \tag{5}$$

Can be found from solving:

$$\det\{[K_{LC}] + [K_{NLC}] - \frac{\pi^2}{a^2}\lfloor G_c \rfloor [I]\} = 0 \tag{6}$$

K_{NLC} holds the additional terms due to nonlinear strains in the core, and G_c contains the loading on the faces and the core per unit width (see Appendix). Later, the results section shows that Case (a) is very close to Case (c), yet has a simpler presentation.

The EHSAPT equations given in the Appendix are for global buckling when n=1, and for wrinkling when n>1. They are also presented for a general material combination and asymmetric geometry.

4 Results and Discussion

The next two sections show results for global buckling and wrinkling, respectively. The global buckling problem examines how the three cases of EHSAPT compare with Elasticity. The next section examines wrinkling using Case (a) of EHSAPT and compares with Elasticity. Allen and HSAPT are also given for comparison where appropriate. All critical loads are normalized with the Euler global buckling critical load defined by P_{E0}, equation (17) in [3].

4.1 Global buckling (n=1)

The global buckling critical loads for a graphite face/glass-phenolic honeycomb soft core (SC) sandwich configuration with $\frac{E_x^c}{E_x^f} < 0.001$ and an E-glass face/balsa wood moderate core (MC) sandwich configurations with $\frac{E_x^c}{E_x^f} > 0.001$ were predicted using Allen, HSAPT, and EHSAPT (3 cases) and compared to Elasticity. Fig. 1 and 2 show the predicted normalized critical loads P_{cr}/P_{E0}, for a range of face sheet thickness to total thickness ratios f/h_{tot}=0.02 to 0.2, for SC and MC configurations, respectively. Differences in solution procedures are indicated next to the theories in the legends. For the SC configuration, all theories match Elasticity. However, the MC configuration reveals differences between the theories. First to be noted is that EHSAPT (Case (b)) is very inaccurate because the loading parameter of the core never enters the perturbed characteristic equation because the core has only linear axial strains. In order to fix this, either all the loading needs to be divided amongst the face sheets as in Case (a) or nonlinear axial strains in the core need to be included, and is verified by EHSAPT (Case (a) and (c)) always being close to Elasticity. Allen and HSAPT are very close to each other because the E^c_z term does not make a significant contribution to the global buckling of a long beam (in this case: a/h_{tot}=30). Allen and HSAPT are close to Elasticity for thicker face sheets, but diverge from Elasticity for f/h_{tot}<0.1. This implies that the in-plane rigidity of the core plays a more significant role when the face sheets are very thin relative to the total thickness of the sandwich. Since the EHSAPT Case (a) approach is simple and accurate, it is used in the next section for the study of wrinkling.

4.2 Wrinkling (n>1)

Sandwich composites are subject to face sheet wrinkling as the thickness of the face sheets become very small compared to that of the core. An Elasticity benchmark [6] was used to determine the accuracy of HSAPT and EHSAPT (Case a), for the same f/h_{tot} and isotropic and orthotropic material selections as in [6]. The studied thickness geometric ratio

f/h_{tot} was for {0.01, 0.02, 0.03, 0.04, and 0.05}. Tables 1 through 4 show the normalized critical loads, error, and the wrinkling mode number. Tables 1 and 2 are for isotropic faces and core of E^f/E^c=1000 and 500, respectively, and Tables 3 and 4 are for orthotropic faces and isotropic core, E-glass/polyester unidirectional facings with PVC foam core (E^f_1/E^c~500), and graphite/epoxy unidirectional facings with hexagonal glass/phenolic honeycomb core (E^f_1/E^c~5,000), respectively. Elasticity predicts wrinkling modes for smaller f/h_{tot}, i.e. very thin faces. The global buckling analysis showed that HSAPT becomes less accurate for very thin faces, and this trend is seen again for the wrinkling analysis, with HSAPT giving up to 70% error for f/h_{tot}=0.01 and E^f/E^c=500 (Table 2). Notice that when isolated in-plane rigidities of the face sheets and the core are of the same order and the response depends on the isolated rigidities of the constituents of the sandwich panel, i.e. wrinkling, the computational model that considers all these rigidities, such as the EHSAPT, yields reliable results. For this demanding case, EHSAPT has 12% error. For other material configurations with f/h_{tot}=0.01, EHAPT is always less than 10% in error, even less than 1% for the graphite facings and glass/phenolic core (Table 4). As the faces become thicker (f/h_{tot} increases), the sandwich globally buckles, HSAPT and EHSAPT converge, with EHSAPT closer to Elasticity.

5 Conclusions

The characteristics of the EHSAPT are presented. A simple case study of global buckling of a S-S sandwich beam is used to compare three higher order shear deformable theories (Allen, HSAPT, and 3 solution approach of EHSAPT) with Elasticity. All three high-order theories match Elasticity well for the SC sandwich, while the EHSAPT (Case (a) and (c)) is the only theory to predict Elasticity for MC sandwich with very thin faces. Another study of wrinkling of a S-S sandwich beam with HSAPT and EHSAPT (Case (a)) compared to Elasticity revealed that the in-plane rigidity plays a significant role in predicting high order wrinkling critical loads for very thin face sheets for soft and moderate core sandwich configurations.

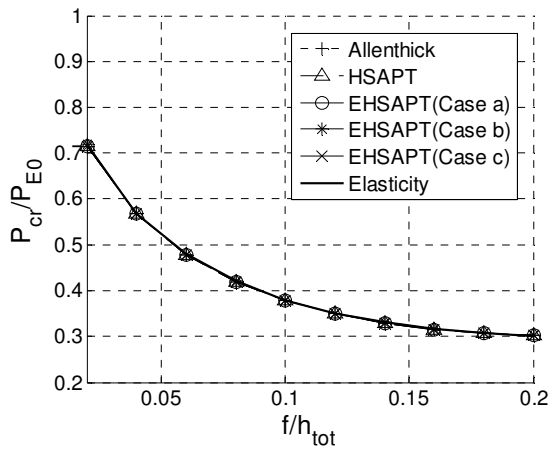

Fig. 1. Normalized critical load of different high-order theories and Elasticity for the SC sandwich configuration. a/h_{tot}=30.

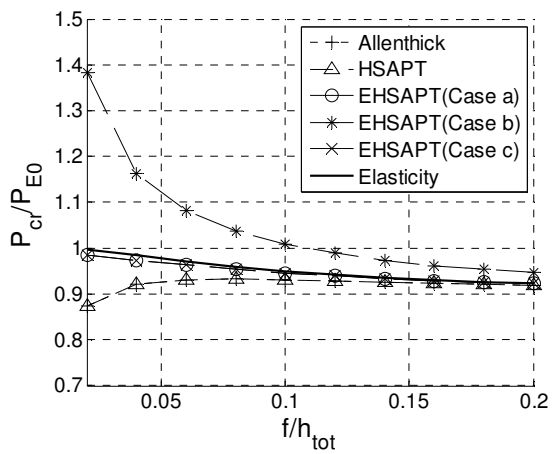

Fig. 2. Normalized critical load of different high-order theories and Elasticity for the MC sandwich configuration

Table 1 Critical loads for Ef/Ec=1,000; normalized with the Euler load (w/o shear). W=wrinkling (multi-wave); GL=global (Euler). Similar to Table 1 in [6].

f/h_{tot}	Elasticity (m)	HSAPT (m)	EHSAPT (m)
	(% difference from Elasticity)		
0.01 Antisymm	0.07381 (24) (W)	0.02654 (20) -(64.0%)	0.07909 (22) (7.2%)
0.02 Antisymm	0.07393 (12) (W)	0.03902 (12) -(47.2%)	0.07080 (12) -(4.2%)
0.03 Antisymm	0.07288 (7) (W)	0.04945 (9) -(32.1%)	0.06967 (8) -(4.4%)
0.04 Antisymm	0.06489 (1) (GL)	0.05900 (7) -(9.1%)	0.06389 (1) -(1.5%)
0.05 Antisymm	0.05411 (1) (GL)	0.05336 (1) -(1.4%)	0.05336 (1) -(1.4%)

Table 2 Critical loads for Ef/Ec=500; normalized with the Euler load (w/o shear). W=wrinkling (multi-wave); GL=global (Euler). Similar to Table 2 in [6].

f/h	Elasticity (m)	HSAPT (m)	EHSAPT (m)
	(% difference from Elasticity)		
0.01 Antisymm	0.12220 (30) (W)	0.03696 (24) -(69.8%)	0.13697 (26) (12.1%)
0.02 Antisymm	0.12100 (15) (W)	0.05477 (14) -(54.7%)	0.11618 (15) -(4.0%)
0.03 Antisymm	0.12110 (10) (W)	0.06985 (11) -(42.3%)	0.11430 (10) -(5.6%)
0.04 Antisymm	0.11800 (6) (W)	0.08361 (9) -(29.1%)	0.11282 (7) -(4.4%)
0.05 Antisymm	0.10270 (1) (GL)	0.09623 (7) -(6.3%)	0.10029 (1) -(2.3%)

Table 3 Critical loads for Ef1/Ec~500; normalized with the Euler load (w/o shear). W=wrinkling (multi-wave); GL=global (Euler). Similar to Table 3 in [6].

f/h	Elasticity (m)	HSAPT (m)	EHSAPT (m)
	(% difference from Elasticity)		
0.01 Antisymm	0.10230 (30) (W)	0.03586 (23) -(65.0%)	0.10775 (25) (5.3%)
0.02 Antisymm	0.10120 (15) (W)	0.05307 (14) -(47.6%)	0.09593 (14) -(5.2%)
0.03 Antisymm	0.10080 (9) (W)	0.06751 (10) -(33.0%)	0.09533 (9) -(5.4%)
0.04 Antisymm	0.09096 (1) (GL)	0.08080 (8) -(11.2%)	0.08953 (1) -(1.6%)
0.05 Antisymm	0.07569 (1) (GL)	0.07486 (1) -(1.1%)	0.07495 (1) -(1.0%)

Table 4 Critical loads for Ef/Ec~5,000; normalized with the Euler load (w/o shear). W=wrinkling (multi-wave); GL=global (Euler). Similar to Table 4 in [6].

f/h	Elasticity (m)	HSAPT (m)	EHSAPT (m)
	(% difference from Elasticity)		
0.01 Antisymm	0.07037 (26) (W)	0.03947 (24) -(43.9%)	0.07099 (25) (0.9%)
0.02 Antisymm	0.06552 (1) (GL)	0.05773 (14) -(11.9%)	0.06506 (9) -(0.7%)
0.03 Antisymm	0.04576 (1) (GL)	0.04558 (1) -(0.4%)	0.04559 (1) -(0.4%)
0.04 Antisymm	0.03577 (1) (GL)	0.03564 (1) -(0.4%)	0.03564 (1) -(0.4%)
0.05 Antisymm	0.02988 (1) (GL)	0.02978 (1) -(0.3%)	0.02978 (1) -(0.3%)

References

[1] Wang, E., Gardner, N. and Shukla, A. "The blast resistance of sandwich composites with stepwise graded cores". *International Journal of Solids and Structures*, Vol. 46, No. 18-19, pp 3492-502, Sept. 2009.

[2] Frostig Y., Baruch M. "High-order buckling analysis of sandwich beams with Transversely flexible core". *Journal of ASCE, EM Division,* Vol. 119, No. 3, pp .476-495, March 1993.

[3] Kardomateas, G. A. "An elasticity solution for the global buckling of sandwich beams/wide panels with orthotropic phases". *Journal of Applied Mechanics,* Vol. 77, No. 2, March 2010.

[4] Carlsson, L. A., and Kardomateas, G. A. Structural and Failure Mechanics of Sandwich Composites. Springer (in press), 2010

[5] Allen, H. G., 1969, *Analysis and Design of Structural Sandwich Panels,* Pergamon, Oxford, Chap. 8.

[6] Kardomateas, G. A. "Wrinkling of wide sandwich panels/beams with orthotropic phases by an elasticity approach". *Journal of Applied Mechanics,* Vol. 72, Nov. 2005

[7] Frostig, Y. "On wrinkling of a sandwich panel with a compliant core and self-equilibrated loads." 9th Intl. Conf. on Sandwich Structures, June 2010.

Appendix

EHSAPT Case (a):

$$[K_{LC}]=\begin{bmatrix} k_{11} & k_{12} & k_{13} & k_{14} & k_{15} & k_{16} & k_{17} \\ k_{12} & k_{22} & k_{23} & k_{24} & k_{25} & k_{26} & k_{27} \\ k_{13} & k_{23} & k_{33} & k_{34} & k_{35} & k_{36} & k_{37} \\ k_{14} & k_{24} & k_{34} & k_{44} & k_{45} & k_{46} & k_{47} \\ k_{15} & k_{25} & k_{35} & k_{45} & k_{55} & k_{56} & k_{57} \\ k_{16} & k_{26} & k_{36} & k_{46} & k_{56} & k_{66} & k_{67} \\ k_{17} & k_{27} & k_{37} & k_{47} & k_{57} & k_{67} & k_{77} \end{bmatrix} \tag{7}$$

Where,

$$k_{11}=\frac{47\,C_{55}^c}{30c}+\frac{6c\,\alpha^2 C_{11}^c}{35}+C_{11}^b f_b\,\alpha^2,$$

$$k_{12}=-\frac{4\,C_{55}^c}{3c}+\frac{2c\,\alpha^2 C_{11}^c}{15},\quad k_{13}=\frac{4\,C_{55}^c}{5}-\frac{2c^2\,\alpha^2 C_{11}^c}{35},$$

$$k_{14}=-\frac{7\,C_{55}^c}{30c}+\frac{c\,\alpha^2 C_{11}^c}{35},\quad k_{15}=-\frac{3\,c\,f_b\alpha^3 C_{11}^c}{35}-\alpha\eta_{b3},$$

$$k_{16}=-\alpha\beta_1;\quad k_{17}=\frac{3\,c\,f_t\,\alpha^3 C_{11}^c}{70}+\alpha\eta_{t2},$$

$$k_{22}=\frac{8\,C_{55}^c}{3c}+\frac{16c\,\alpha^2 C_{11}^c}{15},\quad k_{23}=0,\quad k_{24}=k_{12},$$

$$k_{25}=-\frac{c\,f_b\alpha^3\,C_{11}^c}{15}+\alpha\eta_{b6},\quad k_{26}=0,$$

$$k_{27}=\frac{c\,f_t\,\alpha^3 C_{11}^c}{15}-\alpha\eta_{t6},\quad k_{33}=\frac{8c\left(21\,C_{55}^c+2c^2\alpha^2 C_{11}^c\right)}{105},$$

$$k_{34}=\frac{2\left(-14\,C_{55}^c+c^2\alpha^2 C_{11}^c\right)}{35},\quad k_{35}=\frac{c^2 f_b\alpha^3 C_{11}^c}{35}-\alpha\eta_{b4},$$

$$k_{36}=\alpha\beta_3,\quad k_{37}=\frac{c^2 f_t\alpha^3 C_{11}^c}{35}-\alpha\eta_{t4},$$

$$k_{44}=\frac{47\,C_{55}^c}{30c}+\frac{6c\,\alpha^2 C_{11}^c}{35}+C_{11}^t f_t\alpha^2,\quad k_{45}=-\frac{c\,f_b\,\alpha^3 C_{11}^c}{70}-\alpha\eta_{b2},$$

$$k_{46}=\alpha\beta_1, k_{47}=\frac{3cf_t\alpha^3 C_{11}^c}{35}+\alpha\eta_{t3},$$

$$k_{55}=\frac{7\,C_{33}^c}{6c}+\frac{3c\,f_b^2\,\alpha^4 C_{11}^c}{70}+\frac{f_b^3\,\alpha^4 C_{11}^b}{12}-\alpha^2\eta_{b8},$$

$$k_{56}=-\frac{4\,C_{33}^c}{3c}-\alpha^2\eta_{b7}, k_{57}=\frac{C_{33}^c}{6c}-\frac{c\,f_b f_t\,\alpha^4 C_{11}^c}{140}-\alpha^2\beta_2,$$

$$k_{66}=\frac{8\,C_{33}^c}{3c}+\frac{16c\,\alpha^2 C_{55}^c}{15}, k_{67}=-\frac{4\,C_{33}^c}{3c}-\alpha^2\eta_{t7},$$

$$k_{77}=\frac{7\,C_{33}^c}{6c}+\frac{3c\,f_t^2\,\alpha^4 C_{11}^c}{70}+\frac{f_t^3\,\alpha^4 C_{11}^t}{12}-\alpha^2\eta_{t8},\quad \alpha=\frac{n\pi}{a} \tag{8}$$

material and geometry constants η's and β's are given in [4],

$$G_a = diag\begin{bmatrix}0 & 0 & 0 & 0 & \kappa^b P & 0 & \kappa^t P\end{bmatrix} \tag{9}$$

$$\kappa^i=\frac{C_{11}^i f_i}{C_{11}^b f_b+C_{11}^t f_t},\qquad \text{for } i=t,b \tag{10}$$

EHSAPT Case (b):

$$G_b = diag\begin{bmatrix}0 & 0 & 0 & 0 & \kappa^b P & 0 & \kappa^t P\end{bmatrix} \tag{11}$$

$$\kappa^i=\frac{C_{11}^i f_i}{2c\,C_{11}^c+C_{11}^b f_b+C_{11}^t f_t}\quad i=t,b \tag{12}$$

EHSAPT Case (c):

$$[K_{NLC}]=\frac{\alpha^2\left(c\,C_{11}^c u_{p,x}+C_{13}^c w_p\right)}{15}\begin{bmatrix} 0&0&0&0&0&0&0\\ 0&0&0&0&0&0&0\\ 0&0&0&0&0&0&0\\ 0&0&0&0&0&0&0\\ 0&0&0&0&4&2&-1\\ 0&0&0&0&2&-14&2\\ 0&0&0&0&-1&2&4 \end{bmatrix} \tag{13}$$

$$G_c = diag\begin{bmatrix}0 & 0 & 0 & 0 & \kappa^b P & \kappa^c P & \kappa^t P\end{bmatrix} \tag{14}$$

$$\kappa^c=\frac{2cC_{11}^c}{2c\,C_{11}^c+C_{11}^b f_b+C_{11}^t f_t},$$

$$\kappa^i=\frac{C_{11}^i f_i}{2c\,C_{11}^c+C_{11}^b f_b+C_{11}^t f_t}\quad i=t,b \tag{15}$$

$$u_p(x)=-\frac{\kappa^t P}{C_{11}^t}x=-\frac{\kappa^b P}{C_{11}^b}x=-\frac{\kappa^c P}{C_{11}^c}x$$

$$w_p(x)=-\frac{c\,C_{33}^c}{C_{33}^c}u_{p,x} \tag{16}$$